

Decision Feedback-Aided Known-Interference Cancellation

Karel Pärlin, Aaron Byman, Tommi Meriläinen, and Taneli Riihonen

Abstract—Known-interference cancellation (KIC) in combination with cooperative jamming can be used to provide covertness and security to wireless communications at the physical layer. However, since the signal of interest (SI) of a wireless communication system acts as estimation noise, i.e., interference, to KIC, the SI limits the extent to which the known interference (KI) can be canceled and that in turn limits the throughput of the wireless communication system that is being hidden or secured. In this letter, we analyze a decision feedback-aided known-interference cancellation (DF-KIC) structure in which both the KI and SI are canceled iteratively and successively. Measurement results demonstrate that introducing decision feedback to KIC improves its KI cancellation capability and hence increases the wireless communication system’s useful throughput, albeit at the expense of a higher computational load.

Index Terms—Adaptive filtering, channel estimation, frequency offset, quality of transmission, jamming, electronic warfare.

I. INTRODUCTION

WIRELESS communications are inherently susceptible to adversarial exploits, such as detection and eavesdropping, on the physical layer level. Cooperative jamming and receiver-side KIC are one way to fortify wireless communications against this weakness [1]–[3]. The key challenge in cooperative jamming is interference management and its suppression [4], the latter of which requires at the very least precise time–frequency synchronization and channel estimation [5]–[8] but can also benefit from estimating other hardware impairments [9]–[11]. Numerous works on KIC have demonstrated the feasibility of estimating and compensating for these aspects relying on different sets of hardware operating in both laboratory and outdoor conditions [2], [3], [7], [10], [12], [13]. However, as the KI propagation path modeling becomes sufficiently accurate, in certain cases the limiting factor to KIC becomes instead the SI, since the SI ultimately acts as estimation noise to the adaptive KI cancellation. This will prevent the post-KIC channel capacity from reaching that what would be achieved without cooperative jamming.

This work has been submitted to the IEEE for possible publication. Copyright may be transferred without notice, after which this version may no longer be accessible.

This research work was supported by the Research Council of Finland and the Finnish Research Impact Foundation.

K. Pärlin and T. Riihonen are with Tampere University, Faculty of Information Technology and Communication Sciences, Korkeakoulunkatu 1, 33720 Tampere, Finland (e-mail: karel.parlin@tuni.fi; taneli.riihonen@tuni.fi).

A. Byman and T. Meriläinen are with Bittium Wireless, Ritarharjuntie 1, 90590 Oulu, Finland (e-mail: aaron.byman@bittium.com; tommi.merilainen@bittium.com).

One way to approach the post-KIC residual KI, and to approach interference from a wireless communications perspective in general, is to adapt the SI transmission rate to match what the interference-included channel capacity facilitates [14], [15]. However, this will of course decrease the communication system’s throughput [16]. The alternative way is to try to reduce the impact that the different received signals have on one another in their respective processing stages. Since the output of a receiver is an estimate of the transmitted SI symbols, that estimate can be typically used to reconstruct a replica of the transmitted SI waveform, which can then be suppressed in the received signal like the KI [17]. If any of the initial estimates of the transmitted SI symbols are erroneous, which assumedly is the case, since otherwise improving KIC would not be necessary, such decision feedback-aided filtering has of course the possibility of error propagation.

Still, in many cases the methods with decision feedback outperform those without it, e.g., in narrowband interference cancellation [18]–[22], in channel equalization [23]–[25], and in multi-user interference cancellation [26]–[28]. In this letter, we therefore propose a DF-KIC method that iteratively cancels both the received KI and SI, whereas the transmitted digital waveform of the former is known completely *a priori* and the latter is of a known structure, e.g., OFDM, but contains unknown data. We demonstrate the method’s performance in comparison to that without decision feedback based on laboratory measurements carried out with commercial off-the-shelf software-defined radios (SDRs) and using SIs with different signal-to-interference-and-noise ratio (SINR) requirements.

II. KNOWN-INTERFERENCE CANCELLATION

A. System Model and Base Known-Interference Cancellation

The KI and SI transmitters broadcast signals $x(n)$ and $s(n)$, respectively, the former of which is known *a priori* to only authorized receivers and the latter of which is unknown but of interest to both authorized and unauthorized receivers. Then, the superposed signal at any receiver becomes

$$d(n) = \mathbf{w}_n^H \mathbf{y}_n e^{j\phi^x(n)} + \mathbf{h}_n^H \mathbf{z}_n e^{j\phi^s(n)} + v(n), \quad (1)$$

where \mathbf{w}_n and \mathbf{h}_n are the channel impulse responses from the KI and SI transmitters to the receiver, respectively, $\{\cdot\}^H$ denotes conjugate transpose, $v(n)$ is measurement noise with variance σ_v^2 , \mathbf{y}_n and \mathbf{z}_n account for $x(n)$ and $s(n)$ with time-varying sampling frequency offsets $\eta^x(n)$ and $\eta^s(n)$ according in [8, Eq. (2)], and the multiplicative terms $e^{j\phi^x(n)} = e^{j\sum_{i=1}^n \epsilon^x(i)}$ and $e^{j\phi^s(n)} = e^{j\sum_{i=1}^n \epsilon^s(i)}$ account for the carrier frequency offsets and phase noise.

Not knowing $x(n)$, any unauthorized receiver is left with the superposition of the signals. Authorized receivers, however, can suppress $x(n)$ from the received signal so that

$$e(n) = d(n) - \hat{\mathbf{w}}_n^H \hat{\mathbf{y}}_n e^{j\hat{\phi}^x(n)} \stackrel{\text{ideally}}{=} \mathbf{h}_n^H \mathbf{z}_n e^{j\phi^s(n)} + v(n), \quad (2)$$

where \hat{w}_n , $\hat{\epsilon}^x(n)$, and $\hat{\eta}^x(n)$ are, respectively, accurate estimates of the channel impulse response, carrier frequency offset, and sampling frequency offset at iteration n , $e^{j\hat{\phi}^x(n)} = e^{j\sum_{i=1}^n \hat{\epsilon}^x(i)}$, and \hat{y}_n is the result of resampling $x(n)$ with $\hat{\eta}^x(n)$. In practice, estimation inaccuracies mean that some residual KI will typically remain in (2). For the base, i.e., non-decision feedback-aided, KIC we herein use the variable step sizes frequency offsets-compensated least mean squares (VSS-FO-LMS) algorithm, which iteratively updates its estimates \hat{w}_n , $\hat{\epsilon}^x(n)$, and $\hat{\eta}^x(n)$ by minimizing the error in (2) based on stochastic gradient descent (SGD) rules [29, Algorithm 1].

B. Known-Interference Cancellation with Decision Feedback

The DF-KIC steps are listed as Algorithm 1 and its structure is illustrated in Fig. 1. The algorithm operates over an entire received SI frame and assumes that the start of the frame has been located outside of DF-KIC (e.g., by relying on a known preamble and/or training symbols). The algorithm begins by initializing the estimated parameter sets ζ^x and ζ^s related to the KI and SI channels, respectively, by setting the parameter estimates to zero. These sets will be passed across the decision feedback iterations to reduce the VSS-FO-LMS's convergence time, analogous to the concept of warm restarts in SGD methods in general [30].

The base KIC is then executed and both the original received signal d and the post-KIC error signal e^x are demodulated. The demodulator is required to provide estimated data symbols r^d and r^e as well as received signal quality indicators δ^d and δ^e . Herein, OFDM with different orders of QAM is used for modulation and nondata-aided error vector magnitude (EVM) [31] is used as the quality indicator. Nondata-aided EVM is typically more optimistic than data-aided EVM but can still provide a useful estimate of the SINR [32], [33]. The quality indicator is relied on to assess which of the demodulated symbol streams, r^d or r^e , is likely to contain less errors, whether that symbol stream is likely to be of sufficient quality for further processing, and whether successive decision feedback iterations improve the post-KIC SINR.

If neither the received signal nor base KIC leads to a satisfactory quality indicator δ^t , the symbol stream with better quality is modulated to reconstruct an estimate \hat{s} of the transmitted SI waveform. That SI estimate is then matched to that received, using the base KIC and the error signal e^x , from which the KI has been canceled, as the desired signal. The resulting estimate of the received SI, denoted as \hat{d}^s , is removed from the total received signal resulting in a SI-reduced received signal e^s . The base KIC is then used again to match the KI to that received based on the SI-reduced received signal. The estimate of the received KI, denoted \hat{d}^x , is removed from the total received signal and the resulting KI-reduced received signal is demodulated, which concludes the decision feedback iteration.

If the stopping criterion δ^t has not been met, if the signal quality indicator has improved, and if the maximum number of decision feedback iterations K have not been reached, then the algorithm proceeds to the next iteration. Note that the VSS-FO-LMS algorithm requires as inputs certain forgetting factors and the number of taps but these are herein assumed to be fixed and are omitted from the algorithm listing for brevity.

Algorithm 1

```

1: procedure DF-KIC( $\mathbf{x}$ ,  $\mathbf{d}$ ,  $K$ ,  $\delta^t$ )
2:    $\zeta^x(0) \leftarrow \{\hat{\mathbf{w}} : \mathbf{0}, \hat{\epsilon}^x : 0, \hat{\eta}^x : 0\}$ 
3:    $\zeta^s(1) \leftarrow \{\hat{\mathbf{h}} : \mathbf{0}, \hat{\epsilon}^s : 0, \hat{\eta}^s : 0\}$ 
4:    $\hat{\mathbf{d}}^x, \zeta^x(1) \leftarrow \text{VSS-FO-LMS } (\mathbf{x}, \mathbf{d}, \zeta^x(0))$ 
5:    $\mathbf{e}^x \leftarrow \mathbf{d} - \hat{\mathbf{d}}^x$ 
6:    $\mathbf{r}^d, \delta^d \leftarrow \text{Demodulator } (\mathbf{d})$ 
7:    $\mathbf{r}_0^e, \delta^e(0) \leftarrow \text{Demodulator } (\mathbf{e}^x)$ 
8:   if  $\delta^e(0) > \delta^d$  then
9:      $\mathbf{r}_0^e \leftarrow \mathbf{r}^d$ 
10:     $\delta^e(0) \leftarrow \delta^d$ 
11:   end if
12:   if  $\delta^e(0) < \delta^t$  then
13:     end procedure
14:   end if
15:   for  $k \leftarrow 1$  to  $K$  do
16:      $\hat{\mathbf{s}} \leftarrow \text{Modulator } (\mathbf{r}_{k-1}^e)$ 
17:      $\hat{\mathbf{d}}^s, \zeta^s(k+1) \leftarrow \text{VSS-FO-LMS } (\hat{\mathbf{s}}, \mathbf{e}^x, \zeta^s(k))$ 
18:      $\mathbf{e}^s \leftarrow \mathbf{d} - \hat{\mathbf{d}}^s$ 
19:      $\hat{\mathbf{d}}^x, \zeta^x(k+1) \leftarrow \text{VSS-FO-LMS } (\mathbf{x}, \mathbf{e}^s, \zeta^x(k))$ 
20:      $\mathbf{e}^x \leftarrow \mathbf{d} - \hat{\mathbf{d}}^x$ 
21:      $\mathbf{r}_k^e, \delta^e(k) \leftarrow \text{Demodulator } (\mathbf{e}^x)$ 
22:     if  $\delta^e(k) < \delta^t$  then
23:       end procedure
24:     else if  $\delta^e(k) > \delta^e(k-1)$  then
25:        $\mathbf{r}_k^e \leftarrow \mathbf{r}_{k-1}^e$ 
26:     end procedure
27:   end if
28:   end for
29: end procedure

```

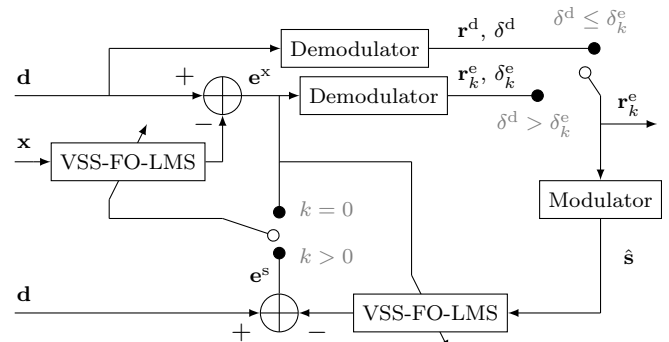
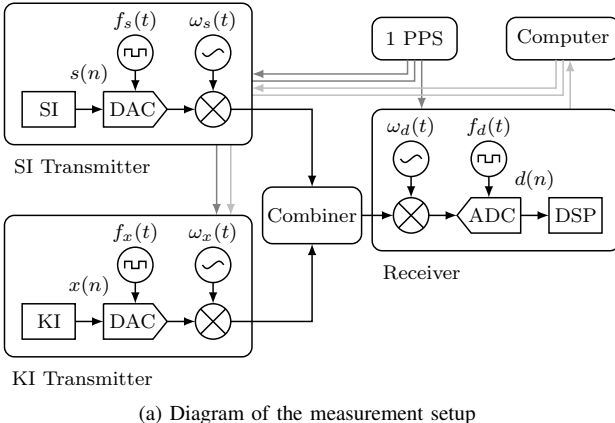


Fig. 1. Structure of DF-KIC for successive cancellation of KI and SI.



(a) Diagram of the measurement setup



(b) Photo of the measurement setup

Fig. 2. Laboratory measurement setup with three USRP-2900 SDRs.

III. MEASUREMENT SETUP

The impact of decision feedback iterations on KIC was studied based on measurements carried out using the laboratory setup illustrated in Fig. 2 and described below. The transmitters and the receiver were implemented using USRP-2900 SDRs, which were connected over cables. A digital intermediate frequency was used to remove the impact of LO leakages and IQ imbalances. Effectively, the SDRs were configured to 875 MHz carrier frequency with 6.5 MHz sampling frequencies. The transmitted KI and SI power levels were varied with 2 dB steps, resulting in measurement grids that cover most practical received SINRs. A reference timing generator was used that provides coarse knowledge about the positions of the KI and SI waveforms in the received signal but does not reduce the carrier nor sampling frequency offsets nor lessen the challenge in estimating them.

The KI was generated using a pseudo-random number generator with normal distribution and then limited to approximately 5 MHz bandwidth. This approach can be straightforwardly adopted in practice to provide authorized receivers, and authorized receivers only, with the means to locally generate the KI that is to be canceled based on a pre-shared secret seed for the pseudo-random number generator. The SI was an OFDM signal composed of 192 subcarriers with 24 kHz spacing, 32 of the subcarriers were used as pilots, and the OFDM symbols were padded with $1/16$ -length cyclic prefixes.

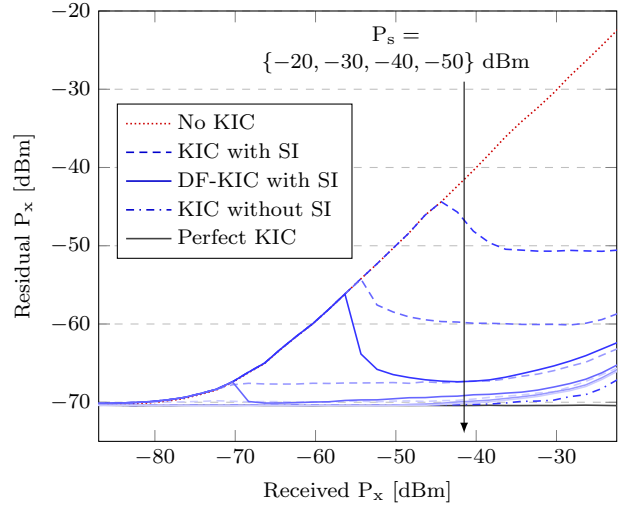


Fig. 3. Basic KIC performance depending on the received KI and SI strength.

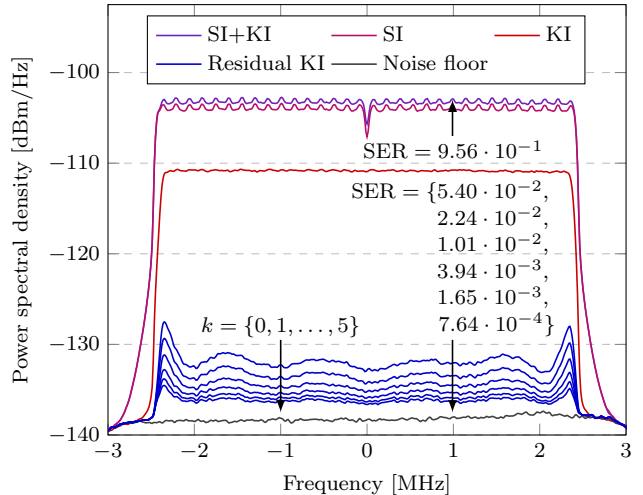


Fig. 4. Power spectral density of KI throughout the DF-KIC iterations.

The data was modulated using either 4-, 8-, 16-, 32-, 64-, 128-, or 256-QAM and the pilots using BPSK. The OFDM symbols were concatenated into five frames of 5000 symbols each, whereas the first symbol of each frame was considered a training symbol known to the receiver. The VSS-FO-LMS forgetting factors were set to $\lambda_e = 0.99995$, $\lambda_R = 0.9995$, $\lambda_y = 0.999$, and $\lambda_e = \lambda_\eta = 0.99999$. $M = 5$ taps were used to model the over-the-cable channels with $K = 8$ maximum number of decision feedback iterations.

IV. MEASUREMENT RESULTS

Fig. 3 illustrates the SI's impact on the base KIC. When no SI is received, the KI is suppressed to the noise floor in most of the analyzed range. Only when the received KI is very powerful does the cancellation become limited by the hardware impairments. However, when a SI is received, the KI suppression is limited because of the interference from the SI. The residual KI power level then depends on that of the received SI, e.g., the results show that when the received SI has

a roughly 50 dB signal-to-noise ratio (SNR), the residual KI after base KIC is at least 20 dB above the noise floor, which, consequently, results in at most 30 dB post-KIC SINR. The residual KI after DF-KIC, however, is at most 8 dB above the noise floor, which results in at most 42 dB post-KIC SINR.

The impact of decision feedback on KIC is further visualized in Fig. 4. In that measurement, the KI and SI are received at -44 dBm and -38 dBm power levels, respectively, and the SI symbols are modulated using 256-QAM. As such, the KI is powerful enough to completely prevent the SI from being demodulated and the SI is powerful enough to prevent the KI from being completely suppressed. Through the decision feedback iterations, the KIC suppresses the residual KI enough for the SI to be demodulated with a SER below 10^{-3} , which we here assume to be sufficiently low for regular post-KIC channel coding to handle the remaining errors.

Fig. 5 shows, depending on the receiver KIC capability and SI modulation order, the received SINRs at which the 10^{-3} SER can be reached and the number of decision feedback iterations that DF-KIC takes on top of the base KIC to reach that target. The SINRs are shown as contour lines and the number of required iterations are shown by the underlying heatmap. Since 4- and 8-QAM have relatively low SINR requirements, the post-KIC SINR after applying only the base KIC once is essentially already sufficient to reach the targeted SER. However, as the modulation order increases, the benefit of DF-KIC over KIC becomes more and more evident, until 128- and 256-QAM, when the base KIC alone is completely inadequate and the decision feedback iterations are indispensable in reaching the targeted SER. The average number of iterations, considering only cases where DF-KIC improves on KIC, is 0, 1, 1.4, 1.5, 1.6, 1.9, and 3.6 for 4-, 8-, 16-, 32-, 64-, 128-, and 256-QAM, respectively.

Finally, Fig. 6 demonstrates the impact of DF-KIC on the communication system's useful throughput through

$$\text{goodput} = (1 - \text{SER}) \cdot \log_2(M^{\text{QAM}}) \cdot R, \quad (3)$$

where M^{QAM} is the modulation order and $R = 3/4$ is the error

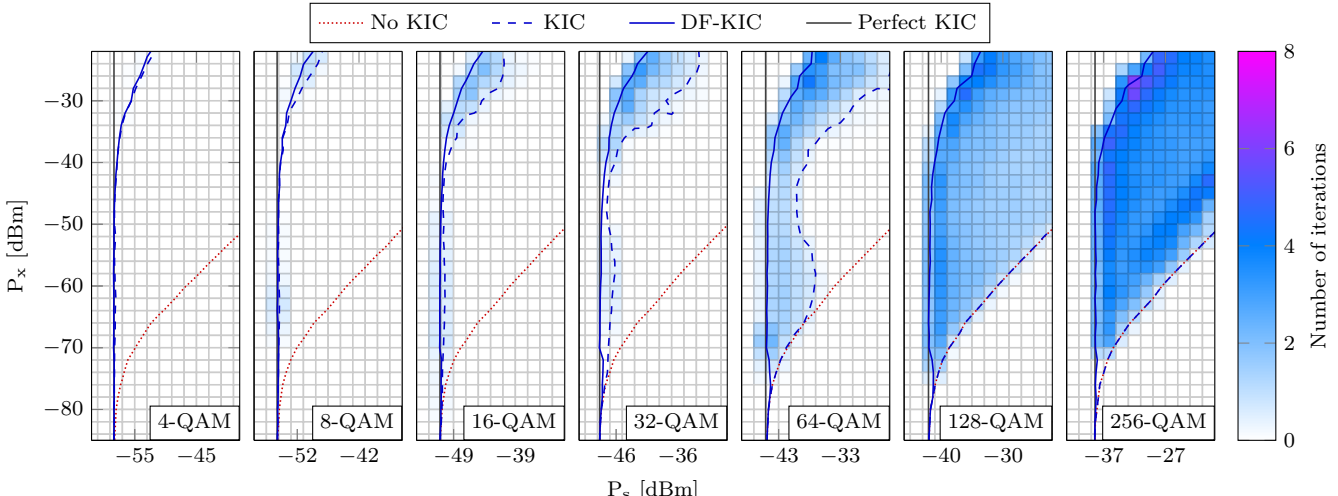


Fig. 5. Received SINR requirements to reach 10^{-3} SER depending on the receiver capabilities and SI modulation order. Also plotted are the number of decision feedback iterations required on average by the DF-KIC to reach a SER of 10^{-3} .

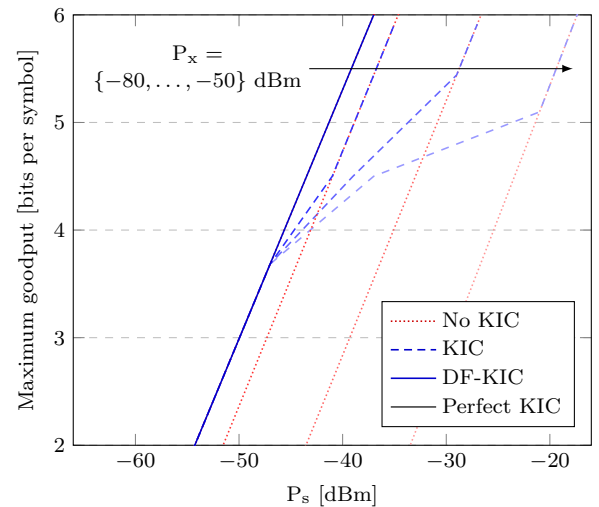


Fig. 6. Maximum achievable useful throughput.

correction coding rate. The results show that when the KI is received weakly relative to the SI, the choice of KIC does not impact the achievable useful throughput (i.e., the resulting plot lines essentially overlap). However, at higher received KI power levels, decision feedback iterations increase the number of useful bits that can be transmitted in a symbol by up to 35%.

V. CONCLUSION

This letter introduced a DF-KIC method that addresses the feasibility of KIC when the received KI and SI are both powerful enough to interfere with the processing of one another. The proposed method iteratively cancels the received KI and SI waveforms, assuming *a priori* knowledge of the transmitted KI and reconstructing the transmitted SI based on that received. Measurement results demonstrate that DF-KIC outperforms basic KIC at many SINRs, leading to lower post-KIC residual KI and SER. The improved performance comes at the expense of additional computational cost.

REFERENCES

- [1] J. M. Hamamreh, H. M. Furqan, and H. Arslan, "Classifications and applications of physical layer security techniques for confidentiality: A comprehensive survey," *IEEE Commun. Surveys Tuts.*, vol. 21, no. 2, pp. 1773–1828, Oct. 2018.
- [2] K. Pärlin, T. Riihonen, M. Turunen, V. Le Nir, and M. Adrat, "Known-interference cancellation in cooperative jamming: Experimental evaluation and benchmark algorithm performance," *IEEE Wireless Commun. Lett.*, vol. 12, pp. 1598–1602, Sep. 2023.
- [3] W. Guo, H. Zhao, and Y. Tang, "Testbed for cooperative jamming cancellation in physical layer security," *IEEE Wireless Commun. Lett.*, vol. 9, no. 2, pp. 240–243, Feb. 2020.
- [4] M. Atallah, G. Kaddoum, and L. Kong, "A survey on cooperative jamming applied to physical layer security," in *Proc. Int. Conf. on Ubiquitous Wireless Broadband*, Oct. 2015.
- [5] W. Guo, H. Zhao, W. Ma, C. Li, Z. Lu, and Y. Tang, "Effect of frequency offset on cooperative jamming cancellation in physical layer security," in *Proc. IEEE Globecom Workshops*, Dec. 2018.
- [6] W. Guo, C. Li, H. Zhao, R. Wen, and Y. Tang, "Comprehensive effects of imperfect synchronization and channel estimation on known interference cancellation," *IEEE Trans. Veh. Technol.*, vol. 69, no. 1, pp. 457–470, Jan. 2020.
- [7] W. Guo, C. Song, X. Xia, F. Hu, H. Zhao, S. Shao, and Y. Tang, "Analysis of cooperative jamming cancellation with imperfect time synchronization in physical layer security," *IEEE Wireless Commun. Lett.*, vol. 10, no. 2, pp. 335–338, Feb. 2021.
- [8] K. Pärlin, T. Riihonen, V. Le Nir, and M. Adrat, "Estimating and tracking wireless channels under carrier and sampling frequency offsets," *IEEE Trans. Signal Process.*, vol. 71, pp. 1053–1066, Mar. 2023.
- [9] Y. He, M. Zhao, W. Guo, H. Zhao, S. Shao, and Y. Tang, "Performance analysis of nonlinear self-interference cancellation with timing error in full-duplex systems," *IEEE Wireless Commun. Lett.*, vol. 10, no. 5, pp. 1075–1078, May 2021.
- [10] K. Pärlin, M. Turunen, A. Byman, T. Meriläinen, V. Le Nir, M. Adrat, and T. Riihonen, "High-power cooperative jamming with nonlinear known-interference cancellation," *IEEE Trans. Aerosp. Electron. Syst.*, Jan. 2025.
- [11] W. Guo, M. Jin, H. Zhao, and S. Shao, "Cooperative jamming cancellation with time-frequency mismatch, IQ imbalance and LO leakage for secure communications," *IEEE Trans. Wireless Commun.*, 2025.
- [12] K. Pärlin, V. Le Nir, T. Meriläinen, A. Byman, M. Adrat, and T. Riihonen, "Wideband cooperative jamming with band-limited known-interference cancellation," in *Proc. IEEE Mil. Commun. Conf.*, Oct. 2024.
- [13] K. Pärlin, A. Byman, T. Meriläinen, and T. Riihonen, "Known-interference cancellation over time-varying Rayleigh-fading channels," in *Proc. IEEE Mil. Commun. Conf.*, Oct. 2025.
- [14] D. J. Love, R. W. Heath, V. K. Lau, D. Gesbert, B. D. Rao, and M. Andrews, "An overview of limited feedback in wireless communication systems," *IEEE J. Sel. Areas Commun.*, vol. 26, no. 8, pp. 1341–1365, Oct. 2008.
- [15] M. K. Hanawal, M. J. Abdel-Rahman, and M. Krunz, "Joint adaptation of frequency hopping and transmission rate for anti-jamming wireless systems," *IEEE Trans. Mobile Comput.*, vol. 15, no. 9, pp. 2247–2259, Sep. 2016.
- [16] X. Qiu and K. Chawla, "On the performance of adaptive modulation in cellular systems," *IEEE Trans. Commun.*, vol. 47, no. 6, pp. 884–895, Jun. 1999.
- [17] L. B. Milstein, "Interference rejection techniques in spread spectrum communications," *Proceedings of the IEEE*, vol. 76, no. 6, pp. 657–671, Jun. 1988.
- [18] J. Ketchum, "Decision feedback techniques for interference cancellation in PN spread spectrum communication systems," in *Proc. IEEE Mil. Commun. Conf.*, vol. 3, Oct. 1984, pp. 559–564.
- [19] F. Takawira and L. Milstein, "Error propagation in decision feedback interference rejection DS spread spectrum systems," in *Proc. IEEE Mil. Commun. Conf.*, Oct. 1987, pp. 934–937.
- [20] B. Shah and G. Saulnier, "Adaptive jammer suppression using decision feedback in a spread-spectrum receiver," in *Proc. IEEE Mil. Commun. Conf.*, Oct. 1988, pp. 989–995.
- [21] M. L. Dukic, Z. D. Stojanovic, and I. S. Stojanovic, "Performance of direct-sequence spread-spectrum receiver using decision feedback and transversal filters for combatting narrowband interference," *IEEE J. Sel. Areas Commun.*, vol. 8, no. 5, pp. 907–914, Jun. 1990.
- [22] J. D. Laster and J. H. Reed, "Interference rejection in digital wireless communications," *IEEE Signal Process. Mag.*, vol. 14, no. 3, pp. 37–62, May 1997.
- [23] D. George, R. Bowen, and J. Storey, "An adaptive decision feedback equalizer," *IEEE Trans. Commun. Technol.*, vol. 19, no. 3, pp. 281–293, Jun. 1971.
- [24] C. A. Belfiore and J. H. Park, "Decision feedback equalization," *Proc. IEEE*, vol. 67, no. 8, pp. 1143–1156, Aug. 1979.
- [25] G. K. Kaleh, "Channel equalization for block transmission systems," *IEEE J. Sel. Areas Commun.*, vol. 13, no. 1, pp. 110–121, Jan. 1995.
- [26] A. Duel-Hallen, J. Holtzman, and Z. Zvonar, "Multiuser detection for CDMA systems," *IEEE Personal Commun. Mag.*, vol. 2, no. 2, pp. 46–58, Apr. 1995.
- [27] X. Wang and H. V. Poor, "Iterative (turbo) soft interference cancellation and decoding for coded CDMA," *IEEE Trans. Commun.*, vol. 47, no. 7, pp. 1046–1061, Jul. 1999.
- [28] J. G. Andrews, "Interference cancellation for cellular systems: a contemporary overview," *IEEE Wireless Commun. Mag.*, vol. 12, no. 2, pp. 19–29, Apr. 2005.
- [29] K. Pärlin, A. Byman, T. Meriläinen, and T. Riihonen, "A variable step sizes frequency offsets-compensated least mean squares algorithm," 2025, submitted for review, preprint on arxiv.org.
- [30] I. Loshchilov and F. Hutter, "SGDR: Stochastic gradient descent with warm restarts," in *Proc. 5th Int. Conf. on Learn. Representations*, Apr. 2017.
- [31] "IEEE recommended practice for estimating the uncertainty in error vector magnitude of measured digitally modulated signals for wireless communications," *IEEE Std 1765-2022*, pp. 1–105, Nov. 2022.
- [32] H. A. Mahmoud and H. Arslan, "Error vector magnitude to SNR conversion for nondata-aided receivers," *IEEE Trans. Wireless Commun.*, vol. 8, no. 5, pp. 2694–2704, May 2009.
- [33] R. Schmogrow, B. Nebendahl, M. Winter, A. Josten, D. Hillerkuss, S. Koenig, J. Meyer, M. Dreschmann, M. Huebner, C. Koos *et al.*, "Error vector magnitude as a performance measure for advanced modulation formats," *IEEE Photon. Technol. Lett.*, vol. 24, no. 1, pp. 61–63, Jan. 2012.